Detection of Nematic–Smectic Phase Transition in a Semiflexible Main-Chain Liquid Crystalline Polymer

S. D. Hudson,*,† A. J. Lovinger, R. G. Larson, and D. D. Davis

AT&T Bell Laboratories, Murray Hill, New Jersey 07974

R. O. Garay‡ and K. Fujishiro

Department of Polymer Science and Engineering, University of Massachusetts, Amherst, Massachusetts 01003

Received May 3, 1993; Revised Manuscript Received July 13, 1993•

ABSTRACT: We investigate the low-temperature phase of a semiflexible liquid crystalline polyester that was previously thought to display only a nematic mesophase. The polymer is the condensation product of 1,10-decanediyldioxybis(benzoyl chloride) and ethoxy-substituted hydroquinone and has a chemical structure that is strictly periodic. Polymers of two different molecular weights were prepared. For these viscous materials, standard techniques for phase identification are problematic; however, rheological studies easily reveal a nematic–smectic transition and pinpoint the transition temperature. According to X-ray diffraction on oriented fibers, both samples exhibit a smectic A mesophase, in which the layer repeat is equal to one-third the molecular repeat. TEM morphological investigation confirms the rheological and X-ray studies and reveals parabolic focal-conic textures, characteristic of smectics. The utility of rheology as a simple indication of a transition to a smectic phase is emphasized.

Introduction

The mesophase transitions of thermotropic polyesters can be reduced through the introduction of flexible units either as spacers along the main chain[1] or as side substituents.[2] The broadest and most convenient temperature range is achieved with flexible spacers (containing at least five atoms) between mesogens comprising three aromatic rings—the range is too narrow if the mesogen has two rings and too high if it has four or more.[3] The simplest units from which mesogens can be assembled are single aromatic rings linked by esters. There are three such units: hydroquinone (Q), *p*-oxybenzoate (O), and terephthalate (T) units. From these, there are four basic types of three-ring mesogens: OTO, OQO, TQT, and QTQ, distinguished by the orientation and placement of the ester linkages in the backbone. These mesogen types, to a large degree, determine the type of mesophase that results: OTO polymers are smectic;[4] the other three are generally nematic.[1,3,5] Some report smectic mesophases with these later backbones,[6] especially when long flexible spacers are used.[7] The true mesophase is often in question, however, because the optical textures obtained are poorly defined.[3] Substituents on the mesogen can also favor, for example, the nematic mesophase.[8] Short substituents broaden the mesophase temperature range,[5] while long ones can narrow it.[9]

In light of these structure–property principles, the polymer for the present study was chosen to yield a broad nematic range at low temperatures,[10] so that it would be suitable for studies of the rheology of thermotropic polymers. Polymers of similar architecture have been the subject of another rheological study.[11]

Before proceeding with rheological studies, it is essential to characterize the phase behavior of the material. Methods to determine phase transitions most commonly include differential scanning calorimetry (DSC) and polarized optical microscopy (POM). However, for polymeric materials, phase identification by POM is often ambiguous, because their high viscosity leads to fine-scaled textures that are difficult to interpret.

The polymer of the present study was first thought to have only a nematic mesophase.[10] The lower-temperature phase was classified as a semicrystalline solid. However, DSC showed the surprising result that the purported mesophase-to-solid transition did not supercool more than the isotropic-to-nematic transition. Motivated by this result and by an unusual morphology that we observed in bulk semicrystalline samples, we undertook the present study, in which we utilize several techniques to understand the phase behavior of this polymer, especially at low temperatures.

Method

The following polymer, whose synthesis has been described in a previous publication,[10] was prepared in 4-g quantities:

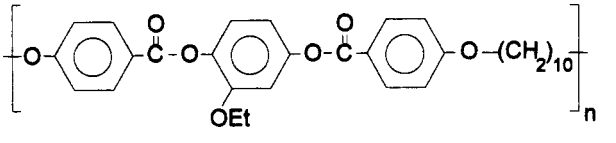

Two different molecular weights were examined: $M_n \sim 5000$ and 30 000 (as determined by GPC).

Thermal characterization was performed on a Perkin-Elmer DSC 7 under N_2 flow at scan rates of typically 10 °C/min. An indium standard was used to calibrate the temperature and energy scales.

Wide-angle X-ray diffraction scans of unoriented samples were obtained at elevated temperatures on a Rigaku system using Ni-filtered Cu Kα radiation. Diffraction patterns of drawn fibers were recorded with a flat-film camera at room temperature.

Rheological characterization was executed on a Rheometrics system IV rheometer, equipped with cone-and-plate fixtures having a 25-mm diameter and a 0.1-rad. cone angle. Vacuum-molded samples were probed with small oscillatory strain, and the elastic and loss dynamic moduli were measured at various temperatures in a N_2 atmosphere.

A Leitz POM equipped with Mettler hot-stage and various video components was used to investigate the texture of polymer

† Present address: Department of Macromolecular Science, Case Western Reserve University, Cleveland, OH 44106.

‡ Present address: Max-Planck-Institut fur Polymerforschung, Ackermannweg 10, Postfach 6500 Mainz, Germany.

• Abstract published in *Advance ACS Abstracts,* September 1, 1993.

0024-9297/93/2226-5643$04.00/0

Table I. Thermal Transitions Detected by DSC (Heating 10 °C/min)

M_n	T_g (°C)	T_{S-N} (°C)	T_{N-I} (°C)
5 000	38	92	192
30 000	46	132	221

films, approximately 3 μm thick, at desired temperatures and thermal/strain histories.

Transmission electron microscopy (TEM) was performed on a JEOL 100CX, operating at 100 kV and equipped with a heating holder, as well as on a JEOL 2000FX operating at 200 kV. Ultrathin films (<100 nm) were prepared in two ways. In one case, a thin film of the polymer was sheared onto a hot glass substrate. The film was removed from this substrate through the use of poly(acrylic acid) (PAA). A 20% solution of PAA in water was cast onto the film and dried in a vacuum oven at 50 °C. When the dried, glassy PAA was removed, the polymer film beneath adhered to it; this film was then backed with carbon to provide mechanical strength necessary before dissolution of the PAA in water. The carbon-coated polymer film was then mounted on 200-mesh Cu screening, from which 3-mm-diameter disks were punched out, and the polymer was then given the desired thermal history before TEM observation.

In the second case, the high surface tension of hot phosphoric acid (compared to that of the molten liquid crystalline polymer) was used to prepare thin films. The material could be quenched to the nematic glass by rapidly pouring the hot acid, with its resident polymer film, onto a room temperature bath of the same acid. After transferring the polymer film to a water surface, it could be retrieved as above with Cu screening. If subsequent thermal treatment was desired, the film was coated with carbon to reinforce it mechanically.

Replicas of semicrystalline bulk specimens were also examined. Slices, approximately 20 μm thick, were obtained using a Reichert-Jung sliding microtome; they were then crystallized by annealing in vacuum at 80 and 90 °C (for the 5K and 30K M_n samples, respectively). The semicrystalline morphology was revealed by selective etching with 40% methylamine in water at room temperature for 3 h. The etch rate is very slow, i.e., ≤50 nm/h. The etched surface was then shadowed with Pt and coated with carbon. After dissolving the polymer in methylene chloride, the Pt–C replica was retained on Cu screening for further TEM examination.

Electron diffraction patterns were further analyzed by densitometry. An aperture of 50 μm was used on an Optronix system P-1000.

Results

Since the phase-transition temperatures are sensitive to molecular weight, they were first determined by DSC, as shown in Table I. The transition temperatures are all decreased by approximately 20 °C for the lower molecular weight, and in both cases the nematic range is very broad (~90 °C). The transition temperatures are sufficiently low that various investigations were possible, as described below. These low temperatures are also desirable for chemical stability of the material. One such chemical reaction which can plague polyesters is transesterification, but, in the range of 100–200 °C, the transesterification rate is negligible. Even if transesterification were to occur, the molecule has been designed such that all ester linkages are equivalent. Therefore, transesterification would cause no chemical changes but could only randomize the molecular-weight distribution.

Further insight into the transitions is gained by examining the DSC traces (Figure 1). If the high-molecular-weight material is cooled at a rate of 10 °C/min, the trace in Figure 1a results. There is a major transition at 210 °C to the nematic phase and a lesser one at 124 °C to the lower-temperature phase, which we will shortly identify as a smectic phase. Finally at 37 °C, the material vitrifies. Comparing these to entries in Table I, we find that the

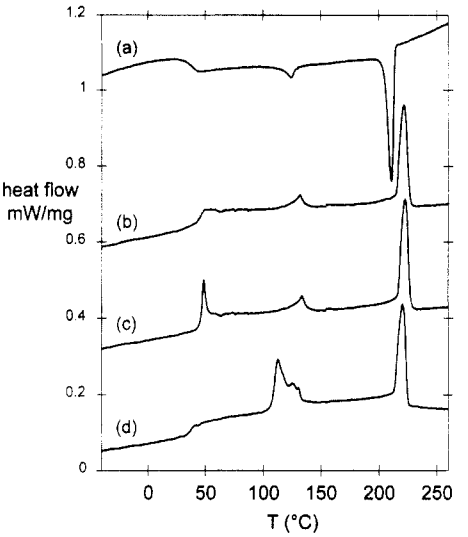

Figure 1. DSC thermograms showing thermal transitions of the high-molecular-weight polymer. All sample weights were 18.8 mg, and all heating/cooling rates are 10 °C/min. (a) Cooling from the isotropic phase. (b) Heating a sample rapidly cooled from the isotropic phase. (c) Heating a sample annealed at 90 °C for 4 days and at 20 °C for 29 days. (d) Heating a sample annealed at 90 °C for 28 days.

supercooling for each of these transitions is similar, about 10 °C. This is the first indication that the lower-temperature phase may not be crystalline, but liquid crystalline.

To probe this question further, we used X-ray diffraction. The diffraction pattern from a fiber drawn from the high-molecular-weight nematic melt (Figure 2a) reveals no crystallinity. The equatorial reflection is broad and diffuse, characteristic of liquidlike lateral packing of polymer chains. Because the diffraction pattern in Figure 2a originates from a highly aligned fiber, the layer-line spacing can be measured. A value of 29.1 Å compares closely to the fully extended repeat spacing of 30.97 Å. Some positioned order is present in this sample, as indicated by the sharp meridional reflection on the third layer line. This conclusion is reinforced by the more diffuse, off-meridional maximum on the first layer line. These two reflections together suggest that neighboring chains are axially displaced by a third of a monomer repeat: the equatorial component of the first layer line peak is $^1/_3$ of the maximum of the equatorial peak. The presence of positional order suggests that the fiber may have transformed to the lower-temperature phase as it cooled during drawing.

Unfortunately, we have not been able to use X-ray diffraction to investigate the difference in structure between smectic and nematic phases, and as a result we cannot confidently assert that the as-drawn specimen is smectic. For example, the features in the diffraction pattern of Figure 2a could arise from pretransitional scattering which may appear in the nematic phase near either a smectic or crystalline phase transition.[12] Such nematics have sometimes been referred to as "cybotactic".[13] X-ray diffraction of unoriented samples has been done at elevated temperatures. Goniometer scans detect only the broad equatorial peak, whose shape and intensity is identical above and below the lower-temperature transition.

Crystallinity can eventually be attained in this material, but only very slowly. After annealing at 90 °C for 72 h, diffraction spots due to polymer crystals are present (Figure 2b). These spots become first perceptible after 4 h at this temperature, but even after 72 h the percent

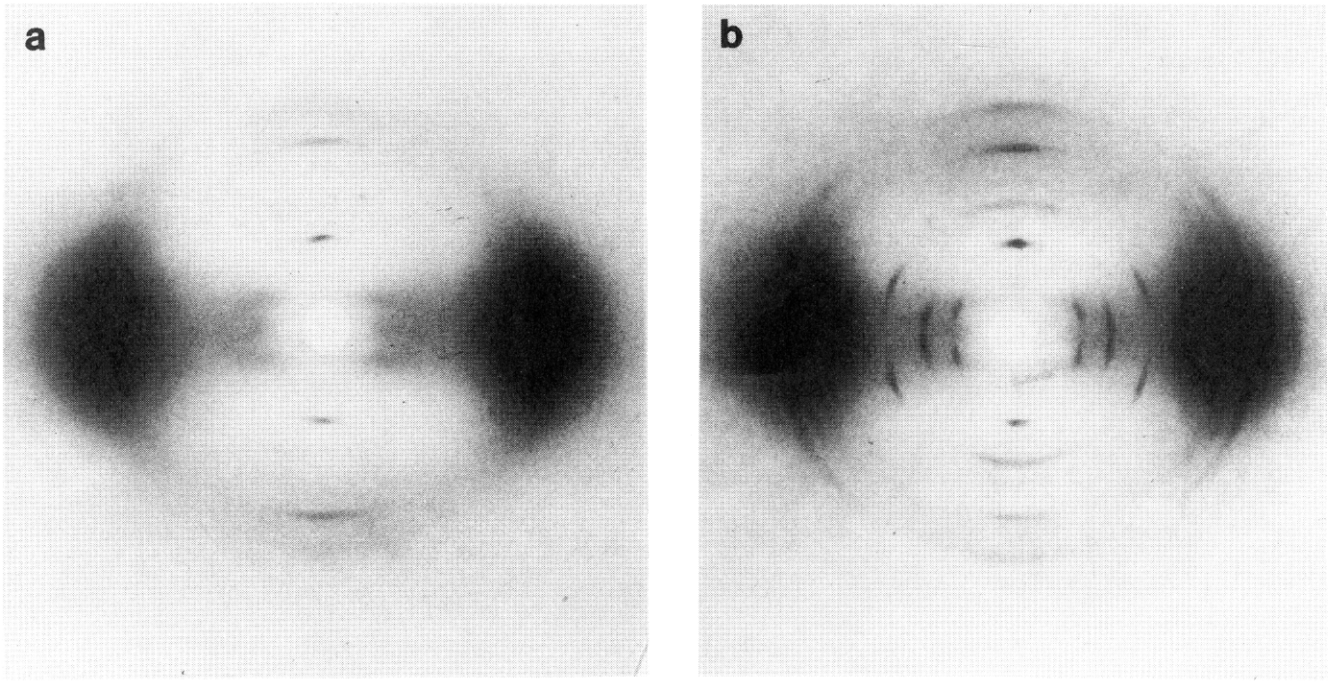

Figure 2. X-ray diffraction patterns of the high-molecular-weight LCP. (a) Fiber drawn from the nematic melt. (b) The same fiber after annealing at 90 °C for 72 h.

crystallinity is small. The crystallization rate is slower still for the lower-molecular weight sample. These slow kinetics prove that the transition detected by DSC at a cooling rate of 10 °C/min does not result from crystallization. The crystallization rate is even much slower in unoriented samples. A goniometer scan of an unoriented sample annealed for 4 days at 90 °C yields no change in the broad equatorial peak. The crystallization rate is retarded, presumably by the bulky and randomly placed ethoxy substituent. The random arrangement of the side chain also leads to very large unit cells and hence to a number of low-angle peaks (Figure 2b).

Having established conditions required for crystallization, our DSC thermograms can be interpreted with confidence. (The following results are all for the higher-molecular-weight polymer. Analogous behavior is also observed for the lower-molecular-weight polymer, yet the transitions are shifted to lower temperatures.) The DSC heating trace of a sample rapidly cooled from the isotropic phase (Figure 1b) mirrors the cooling trace (Figure 1a), indicating that the sample had been quenched to the lower-temperature-mesophase glass. If such a sample is annealed for approximately 4 weeks, an additional melting endotherm is detected. To show that such long anneals are necessary for unoriented material, a sample was annealed for only 4 days at 90 °C and then for 29 days at 20 °C. No additional endotherm above 90 °C was observed (Figure 1c). The mesophase-to-nematic transition remained remarkably unchanged (Figure 1b,c).

Although 4 days at 90 °C was not sufficient, crystallization did take place *from the glass* at 20 °C. When heated to the glass transition, these crystals suddenly melt, giving rise to excess enthalpy (Figure 1c). The excess enthalpy can be eliminated if the sample is not held at room temperature long before calorimetry. When a sample was held at 90 °C for 28 days and then analyzed within a few hours, no excess enthalpy was observed (Figure 1d). On the other hand, a large endotherm comprising three peaks appears between 105 and 135 °C. Both the composite endotherm and the excess enthalpy at the glass transition can be attained if the sample is held sufficiently long at both elevated and room temperatures. (As evidence of stress-induced crystallization in drawn fibers, DSC after only 3 days at 90 °C results in a composite endotherm of similar size and shape to that in Figure 1d.)

The largest of the peaks in the composite endotherm is first at 113 °C. When annealed at 79 °C, this peak appears at 104 °C. Consistent with crystal melting, the temperature of this peak depends on the temperature at which the crystals formed, being 20–25 °C above the annealing temperature. These crystals probably melt to a more highly ordered mesophase than that accessed on cooling, because there is an additional peak at 125 °C. The third endotherm is the previously detected mesophase-to-nematic transition at 132 °C.

Mechanical property measurements give further insight into the nature of this mesophase. The storage modulus, G', was probed at fixed frequency and variable temperature (Figure 3). In the nematic phase, G' increases slowly with decreasing temperature. When the low-temperature phase is reached, G' increases by 2–3 orders of magnitude. The transition is sharp with no observable hysteresis. Therefore, the mechanical measurements allow the lower-temperature transitions to be pinpointed to within ±2 °C; they are 94 and 132 °C, for the low- and high-molecular-weight samples, respectively.

The dynamic moduli were measured as functions of rate and temperature to test for time–temperature superposition. The moduli were shifted by the factor T/T_0, where T_0 is an arbitrary reference temperature, and the frequency was shifted by the factor a_T, determined empirically as the value that best superposed the curves of loss modulus, G'', vs frequency, ω. The shift factors from the nematic phase could be fit with the WLF equation (Figure 4). The

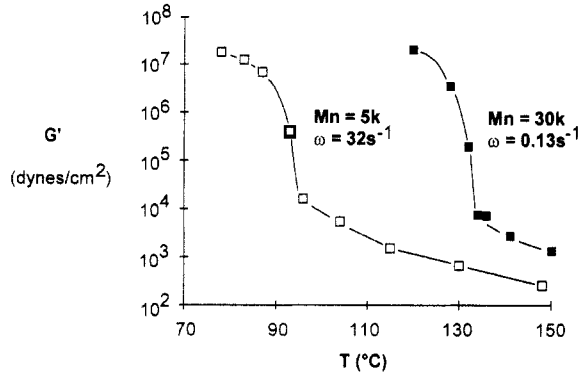

Figure 3. Thermal dependence of the elastic (storage) modulus, G', indicating a sharp rise by 2 orders of magnitude at the nematic-to-smectic transition.

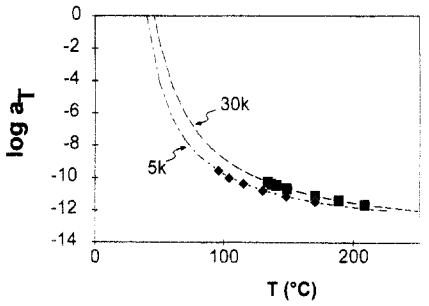

Figure 4. Variation of the shift factor, a_T, with temperature. The symbols denote the empirical shift factors used to superpose the oscillatory data in the nematic phase, while the curves are WLF fits to these data. The two curves are displaced from one another because the glass transition temperature depends on molecular weight.

WLF equation was then used to calculate the shift factors appropriate for the isotropic and the lower-temperature phase. In both of these phases the calculated values for a_T enabled successful superposition of the data (Figure 5). For the 30 000 polymer, the WLF shift factors are $C_1^g = 13.9$ and $C_2^g = 31$. The corresponding values for the low-molecular-weight polymer are 13.5 and 23. These parameter values calculated from the fit are similar to those of other polymers, indicating that the time shifting is related to the onset of the glass transition.

Although the loss modulus superposes in both isotropic and nematic phases, the elastic modulus, G', does not superpose precisely in the nematic phase at low frequencies. Such behavior might be expected since the orientational order parameter of the nematic phase changes with temperature. For a similar reason, the moduli in the smectic phase do not superpose at temperatures within several degrees of the transition, suggesting (in accord with Figure 3) that the smectic positional order parameter is changing rapidly in this temperature range.

After superposing the data, the rheological behavior of the three fluid phases may be compared (Figure 5). The isotropic and nematic phases have power law behavior at low rates. G'' is proportional to ω, which is terminal behavior. G', on the other hand, decays more slowly than is characteristic of terminal behavior, i.e., as $G' \sim \omega^\alpha$, where $\alpha \sim 1.3$–1.4, instead of 2. This result is consistent with that of other nematic polymers.[14]

Power law behavior is not exhibited by the lower-temperature phase. Instead, a low-frequency elastic plateau is observed (Figure 5), characteristic of a gel or network structure. We have already demonstrated by X-ray diffraction that crystallization is not occurring on the time scale of the measurement. This conclusion is confirmed by the rheological studies, which show that a

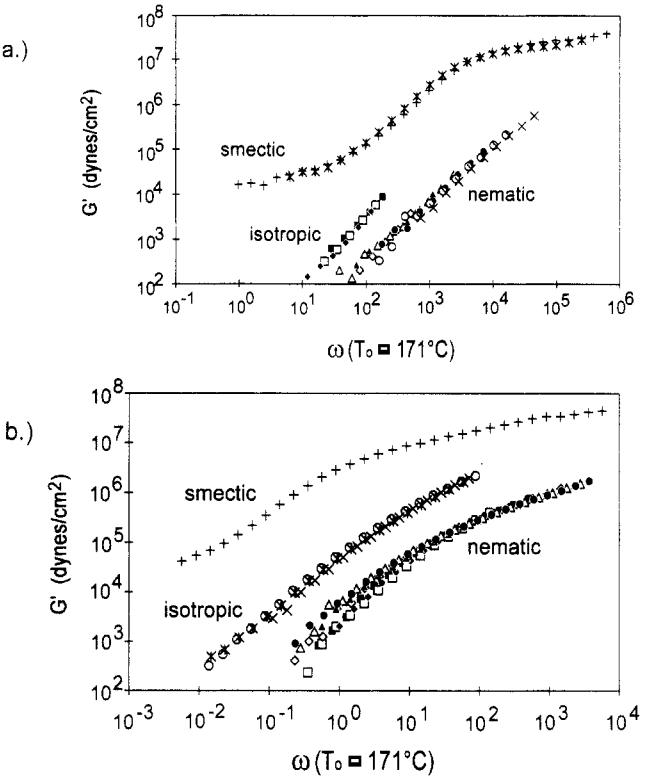

Figure 5. Variation of the elastic modulus, G', as a function of frequency. The frequency axis is shifted in accord with Figure 4. (a) Data for the low-molecular-weight polymer plotted for the following temperatures (°C): 229, 220, 214 (isotropic); 171, 148, 130, 115, 104 (nematic); 83 and 78 (smectic). (b) Corresponding temperatures (°C) for the high-molecular-weight polymer: 250, 240, 230 (isotropic); 209, 189, 171, 149, 141, 137, 134 (nematic); 128 (smectic).

second frequency sweep at the same temperature reproduces the first. When the low-molecular-weight sample was probed at 83 °C, the second sweep, 1.5 h later, reproduced the first sweep exactly at all frequencies. If crystallization were occurring, the low-frequency elastic-plateau modulus would increase with time. Such a change was detected at 78 °C when the second sweep was performed 14 h after the first: the elastic and loss moduli increased at all frequencies by 16% and 12%, respectively. Recent work on other smectic-forming systems, octylcyanobiphenyl (8CB), *n*-nonyl 1-*O*-β-D-glucopyranoside, and lamellar block copolymers, also shows an elastic plateau at low frequencies in the smectic phase.[15] This elastic plateau therefore suggests a smectic (not a cybotactic nematic) mesophase. Furthermore, large-amplitude, low-frequency shear aligns the molecules perpendicular to both the flow and gradient directions. This kind of orientation is similar to that found in other lamellae-forming systems[16,17] and is not expected in nematic fluids.

The smectic transition can also be detected by POM (Figure 6). Figure 6a shows a coarse texture of disclination loops at 120 °C in a sample of the low-molecular-weight material several microns thick. If the sample is rapidly cooled to room temperature, stripes may form within a domain (Figure 6b). These stripes may be erased by returning to the nematic phase. The striped texture was also formed by rapidly cooling to 80 °C. Even though such stripes have been previously observed in other studies,[6,18] their nature or origin is not clear, nor do they form in all samples, but only in those that have very coarse textures. One possibility for the formation of this striped texture may be related to earlier findings of Cladis and Torza,[19] who observed the development of a striped texture during the transition of a nematic-to-smectic transition of

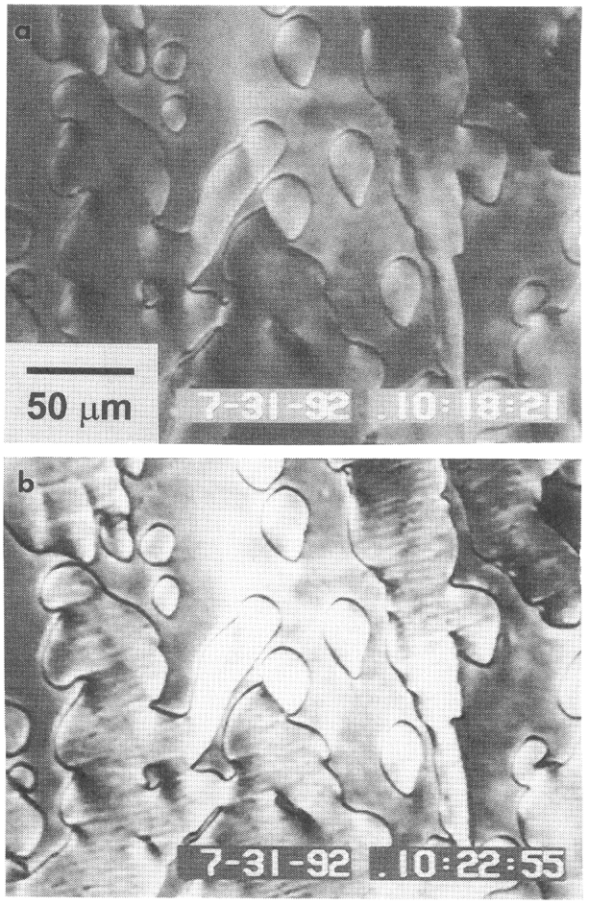

Figure 6. Polarized optical micrographs of the low-molecular-weight polymer showing a texture consisting of a coarse distribution of disclination loops. (a) At 120 °C. (b) After quenching to room temperature.

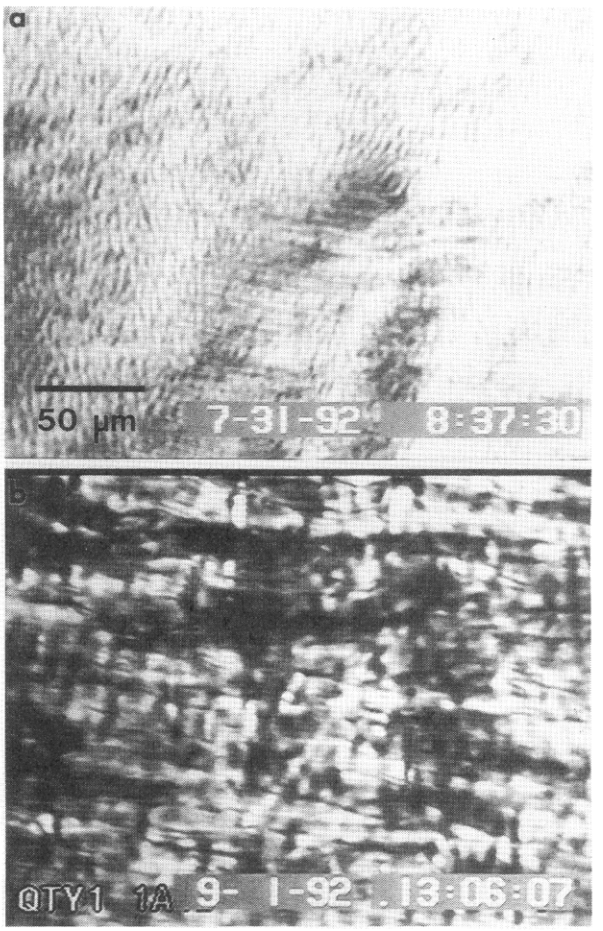

Figure 7. Polarized optical micrographs showing the evolution of texture while holding the specimen temperature at 80 °C. (a) The quenched-in fine-scale banded texture immediately after applied shear. (b) The coarsened texture after 1 month at 80 °C.

a low-molecular-weight liquid crystal. Stripes were not found if the nematic phase was a monodomain, but only if the nematic was bent or distorted. In our samples containing disclinations, the nematic director clearly bends and twists. Thus, if the material becomes smectic, these distortions become highly disfavored and a textural change may take place.

POM observations confirm that the lower-temperature phase is fluid, consistent with smectic order. A sample of the low-molecular-weight polymer was sheared at 120 °C at a rate of $\sim 6\ s^{-1}$. After cessation of shear, finely spaced bands perpendicular to the previous flow direction appeared. Such bands usually form on cessation of shearing of nematic polymers. When the sample was cooled rapidly, this texture remained unchanged and is shown in Figure 7a. When the sample was reheated to 80 °C, the texture coarsened. Of course, the viscosity was high, and the change was not rapid; however, after nearly 1 month at 80 °C, the texture had changed dramatically (Figure 7b). The distortional stresses associated with the fine-scale texture induced by flow were able to relax, as a result of the fluidity of the smectic mesophase.

The most conclusive evidence for a smectic mesophase comes from TEM and electron diffraction. Electron diffraction reveals a clear difference between each of the three phases: semicrystalline, smectic, and nematic (Figure 8). Figure 9 contains the corresponding meridional densitometer traces. In order to obtain quenched nematic films, the cooling rate had to be extremely high. To accomplish this, nematic films that had been spread onto hot phosphoric acid were rapidly quenched to below T_g by pouring the hot acid with nematic film onto a 20 °C bath of the same acid. Since the volume of this bath was 20 times that of the hot acid, the final temperature was approximately 30 °C. Therefore, the film must have been quenched at a rate on the order of 1000 °C/s. Electron-diffraction patterns from such nematic samples have no sharp spots (Figures 8c and 9c). Not visible in this reproduction, but observable on the original negative, are layer lines characteristic of a nematic phase. The visible diffuse equatorial peak results from liquidlike lateral packing. Notably absent is the reflection on the third layer line that was seen in Figure 2a.

To examine the smectic and semicrystalline phases at room temperature, quenching is not so important. Smectic films were prepared by heating C-coated, oriented thin polymer films to the nematic phase (3 min at 150 °C) and cooling to 110 °C for 10 min. Electron diffraction from these samples yields a sharp spot on the third layer line, i.e., the 003 reflection (Figure 9b), but no sharp equatorial peaks (Figure 8b). Also visible in Figure 9b is the 006 meridional reflection. The pattern is similar to the X-ray pattern of the as-drawn fiber (Figure 2a). The layer line spacing indicates, as before, that the chains are nearly extended (Figure 10). Because the first meridional reflection is on the third rather that the first layer line and because the X-ray fiber pattern (Figure 2a) demonstrates that the intensity on the first layer line is off-meridional, the lower-temperature mesophase is smectic-C-like: the layer normal is inclined ~67° to the chain axis, and the resulting spacing is 11.6 Å. On the other hand, the (003) layers are perpendicular to the chain and spaced 9.7 Å.

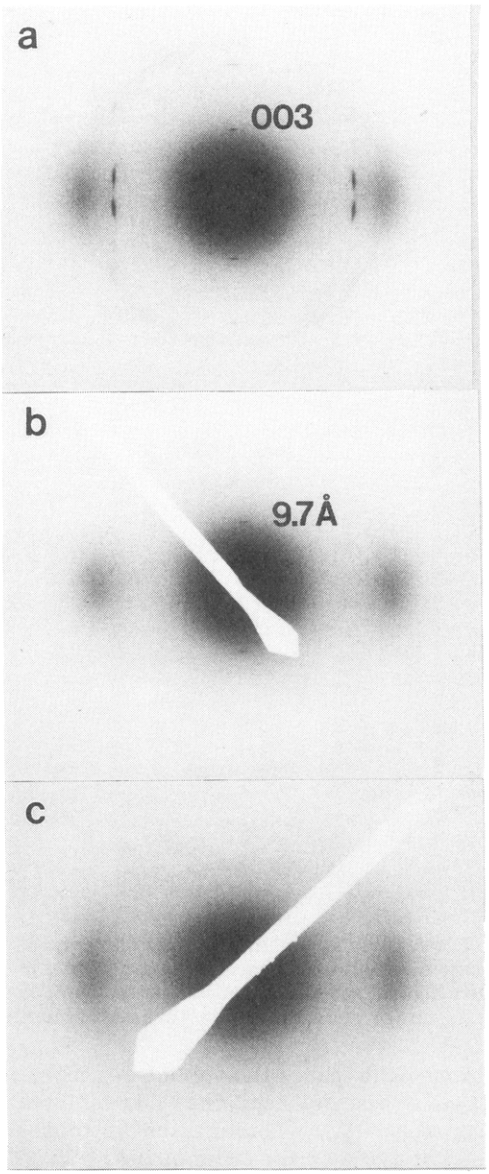

Figure 8. Electron diffraction patterns of samples quenched from (a) the semicrystalline, (b) the smectic, and (c) the nematic phases. See text for sample preparations.

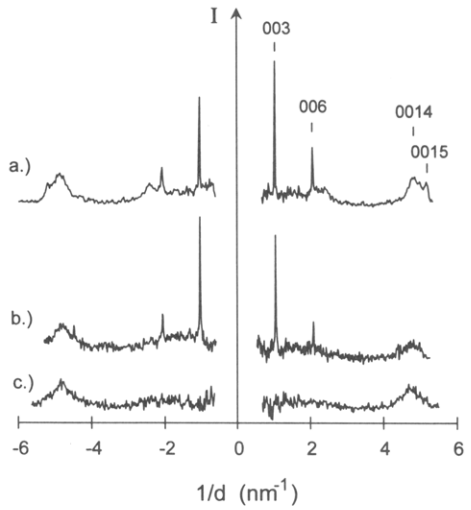

Figure 9. Meridional traces of densitometer scans of the electron diffraction patterns in Figure 8a–c. The Lorentzian inelastic scattering background has been subtracted.[25]

The molecular organization in the smectic mesophase results from packing of the constituent kinked chains

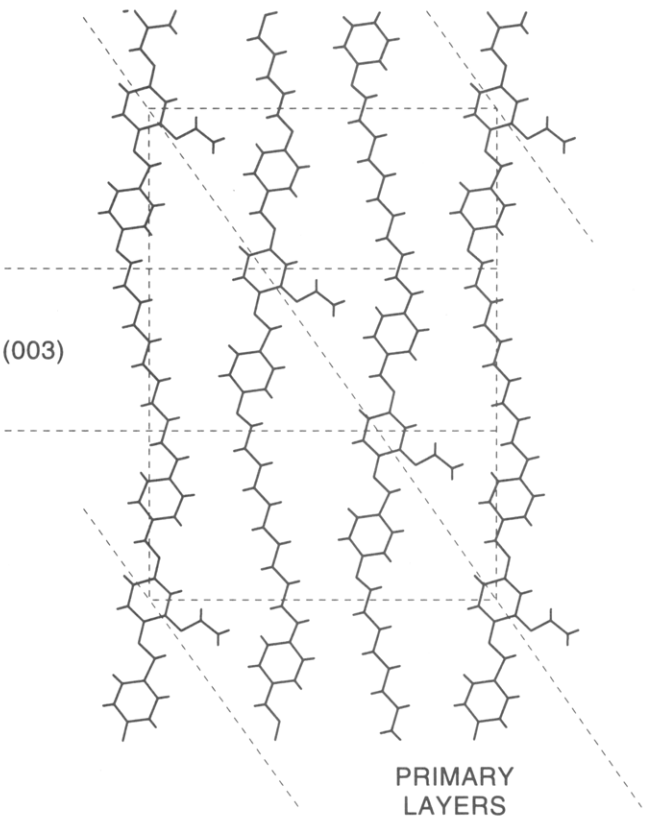

Figure 10. Molecular model of the smectic mesophase.

(Figure 10). Although the 10-carbon spacer must deviate slightly from the all-trans conformation, in order to accommodate the contraction from the fully extended length, such a slight modification will not significantly alter the shape of the molecule. Because of this inherent kink, an axial shift of one-third results in favorable packing of the side group. Such a shift justifies the appearance of the 003 reflection. That the reflection on the first layer line is diffuse is probably indicative of numerous stacking faults that disrupt the long-range order of the primary layers (Figure 9). If stacking faults are such that neighboring molecules are still shifted by one-third, the 003 layers are preserved. Because of this type of disorder, the smectic-C-like mesophase is more accurately classified as smectic A. (An additional source of disorder arises from random placement of the substituent onto the central ring.) Therefore, the relative intensities of the 003 and the first layer-line reflections are accounted for by these simple considerations.

Semicrystalline films were prepared by annealing smectic films for an extended period. A sample was heated to the nematic phase (205 °C) and then cooled to 110 °C; stripes perpendicular to the molecular orientation were observed by POM, indicating transformation to the smectic mesophase. This sample was then held at 90 °C for 65 h to develop crystallinity. Electron diffraction from this sample now yield a new meridional reflection (0015) (Figure 9a) and sharp equatorial spots (Figure 8a), consistent with the X-ray results described previously (Figure 2b). The thin film, however, did not possess fiber symmetry, as verified by tilting the sample about the chain axis. For this reason, fewer equatorial reflections are present in Figure 8a than in Figure 2b.

These three film-processing treatments thus allowed us to isolate successfully each of the phases of the LCP for individual examination by electron diffraction. Our findings were also confirmed by in-situ thermal treatment

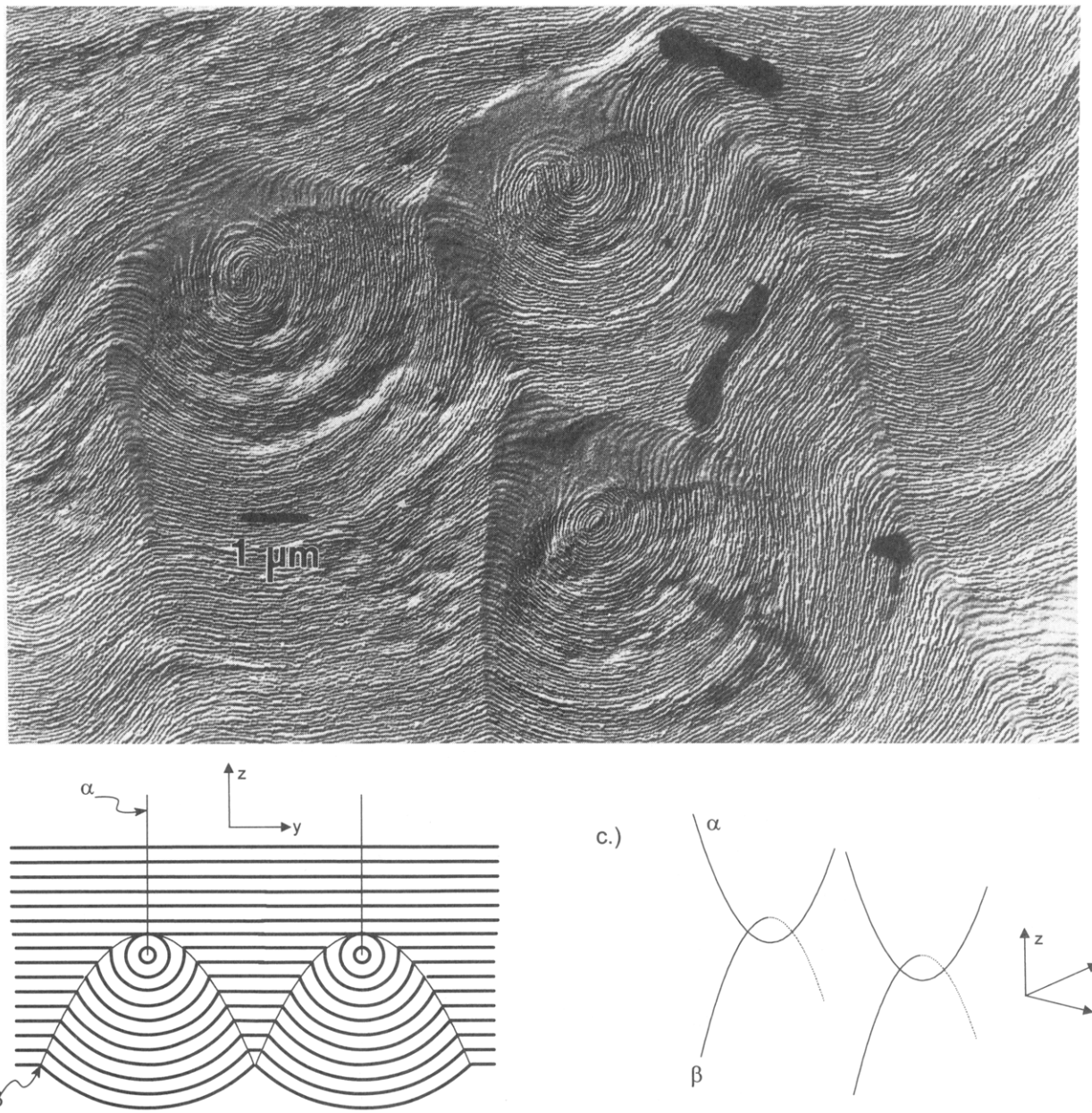

Figure 11. (a, top) TEM replica of a low-molecular-weight polymer specimen treated to reveal the parabolic focal texture (see text for preparation). (b) Two-dimensional schematic of parabolic focal conics. The lamellae are shown as thick lines, and the parabolic cusps (α and β) are shown as hairlines. (c) Three-dimensional view of the arrangement of the parabolic cusps.

of the LCP in the diffraction mode of the TEM. When a semicrystalline film annealed at 90 °C was heated, the sharp equatorial diffraction spots disappeared at 115 °C, consistent with the endotherm obtained in DSC (Figure 1c). However, the 003 reflection remained stable to temperatures as high as 125 °C, indicating disordering to the smectic mesophase before melting to the nematic mesophases. Such disordering behavior produces the complex endothermic peaks detected by DSC (Figure 1c). When the sample was further heated to 156 °C, a nematic pattern consisting of layer lines resulted. Upon cooling back to 60 °C, the 003 smectic reflection returned.

A final confirmation of the smectic mesophase is the texture revealed by TEM. A bulk sample of the lower-molecular-weight polymer was first shear oriented. Subsequently, the material was sliced and annealed in the smectic phase, at a temperature sufficiently low (80 °C) that crystallinity develops. The lamellae form perpendicular to the molecular orientation. The lamellae therefore mark the orientation of the (003) layers characteristic of the smectic mesophase. Focal-conic integer disclinations (cusp singularities) are observed (Figure 11a). In these samples, the disclinations are parabolic in shape and are paired such that they are mutually orthogonal and that the vertex of one intersects the focus of the other[20] (see Figure 11b,c). This texture is characteristic of well-oriented smectic mesophases.

For an excellent description of parabolic focal conics consult Rosenblatt et al.[20] This structure is one limit in the family of Dupin cyclides. A more familiar structure is the opposite extreme: one disclination is a circle and the other a straight line passing through the center of the circle. The lamellae form toroidal surfaces about the circle. These types of defects have been recently observed in aligned lamellar block copolymers.[21] If the circle distorts to an ellipse, the line becomes a hyperbola passing through one of the foci of the ellipse.[22] In the limit of unit ellipticity (when the ellipse is very asymmetric), both the ellipse and the hyperbola become parabolae. The region of high distortion in the parabolic focal-conic texture is confined

to that near the foci, where the smectic layers are multiply connected and form a bridge–tunnel arrangement. As with other Dupin cyclides, the layers form a conical cusp (with local cylindrical symmetry) at the parabola. Parabolic focal conics interact in such a way that they are usually coplanar (Figure 11c). Thus a number of these structures may be observed in the same image (Figure 11a).

Discussion and Conclusions

The presence of a smectic mesophase was revealed in this common thermotropic polyester by a dramatic rheological change, a striped texture in POM, the appearance of a sharp reflection in electron diffraction, and parabolic focal conics in TEM. The typical techniques of DSC, POM, and X-ray diffraction were not sufficient to distinguish this phase from a cybotactic nematic, for example. Rheological characterization is easily done and should be more routine in evaluating the mesophases and transitions of viscous liquid crystalline polymers. Using this method, the transition temperatures were easily pinpointed at 94 and 132 °C for the low- and high-molecular-weight polymers, respectively. The smectic state is revealed by a low-frequency plateau, but great changes over the whole frequency range are easily noted (unlike the side-chain smectic studied by Colby).[23]

In this smectic-A mesophase, the 003 reflection is most intense and has a spacing of 9.7 Å, or one-third the molecular repeat. The smectic-C-like primary layers have a spacing of 11.6 Å and are inclined with respect to the chain axis by 67°. Molecular models indicate this order is related to favorable packing of the kinked backbone, while accommodating the substituent ethoxy.

It is significant that we find a smectic mesophase, since it was previously thought that this polymer exhibited only a nematic mesophase. Its existence also has implications on rheological studies showing evidence of director tumbling.[11] This behavior is thus analogous to that presented by small-molecule liquid crystals, where director tumbling is observed in the nematic phase close to the smectic transition.[24]

At sufficiently low temperatures, the semicrystalline state is most stable. However, the equilibrium melting temperature of the crystals is not known, and, consequently, it is not known whether the smectic is stable or is only metastable. A metastable smectic might always be expected in periodic thermotropes, becoming easier to detect in cases such as this when the crystallization rate is so slow.

In summary, rheological and TEM evidence establish the presence of a smectic mesophase. The low-frequency modulus plateau is characteristic of long-range positional smectic order, and the parabolic focal-conic texture from TEM is its indisputable signature.

References and Notes

(1) Jin, J.-I.; Antoun, S.; Ober, C.; Lenz, R. W. *Br. Polym. J.* **1980**, 132.
(2) Lenz, R. W.; Furukawa, F.; Bhowmik, P.; Garay, R. O.; Majnusz, J. *Polymer* **1991**, *32*, 1703.
(3) Ober, C. K.; Jin, J.-I.; Lenz, R. W. *Adv. Polym. Sci.* **1984**, *59*, 103.
(4) Ober, C.; Jin, J.-I.; Lenz, R. W. *Polym. J.* **1982**, *14*, 9.
(5) Antoun, S.; Lenz, R. W.; Jin, J.-I. *J. Polym. Sci., Polym. Chem. Ed.* **1981**, *19*, 1901.
(6) Campoy, I.; Marco, C.; Gomez, M. A.; Fatou, J. G. *Polym. Bull.* **1991**, *27*, 81.
(7) Strzelecki, L.; vanLuyen, D. *Eur. Polym. J.* **1980**, *16*, 299.
(8) Jo, B.-W.; Jin, J.-I.; Lenz, R. W. *Eur. Polym. J.* **1982**, *18*, 223.
(9) Zhou, Q.-F.; Lenz, R. W. *J. Polym. Sci., Polym. Chem. Ed.* **1983**, *21*, 3313.
(10) Bhowmik, P. K.; Garay, R. O.; Lenz, R. W. *Makromol. Chem.* **1991**, *192*, 415.
(11) Srinivasarao, M.; Garay, R. O.; Winter, H. H.; Stein, R. S. *Mol. Cryst. Liq. Cryst.* **1992**, *222*, 29.
(12) McMillan, W. L. *Phys. Rev. A* **1973**, *8*, 328.
(13) Azaroff, L. V.; Schuman, C. A. *Mol. Cryst. Liq. Cryst.* **1985**, *122*, 309.
(14) Moldenaers, P.; Mewis, J. *J. Rheol.* **1986**, *30*, 567.
(15) Larson, R. G.; Winey, K. I.; Patel, S. S.; Watanabe, H.; Bruinsma, R. *Rheol. Acta*, in press.
(16) Koppi, K. A.; Tirrell, M.; Bates, F. S.; Almdal, K.; Colby, R. H. *J. Phys. II Fr.* **1992**, *2*, 1941.
(17) Patel, S. S.; Larson, R. G.; Winey, K. I.; Watanabe, H. *Macromolecules*, to be submitted.
(18) Chen, S.; Du, C.; Jin, Y.; Qian, R.; Zhou, Q. *Mol. Cryst. Liq. Cryst.* **1990**, *188*, 197.
(19) Cladis, P. E.; Torza, S. *J. Appl. Phys.* **1975**, *46*, 584.
(20) Rosenblatt, C. S.; Pindak, R.; Clark, N. A.; Meyer, R. B. *J. Phys. (Paris)* **1977**, *38*, 1105.
(21) Winey, K. I.; Patel, S. S.; Larson, R. G.; Watanabe, H. *Macromolecules* **1993**, *26*, 2542.
(22) Bouligand, Y. *J. Phys. (Paris)* **1972**, *33*, 525.
(23) Colby, R. H.; Gilmor, J. R.; Galli, G.; Laus, M.; Ober, C. K.; Hall, E. *Liq. Cryst.*, in press.
(24) Cladis, P. E.; Torza, S. *Colloid. Interface Sci.* **1976**, *4*, 487.
(25) Spence, J. C. H. In *High Resolution Transmission Electron Microscopy*; Buseck, P. R., Cowley, J. M., Eyring, L., Eds.; Oxford University Press: Oxford, U.K., 1988; pp 129.